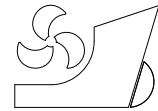


Tianhui Fan  
Dongsheng Qiao  
Jinping Ou



ISSN 0007-215X  
eISSN 1845-5859

## DYNAMIC EFFECTS OF EQUIVALENT TRUNCATED MOORING SYSTEMS FOR A SEMI-SUBMERSIBLE PLATFORM

UDC 629.5(05)

Original scientific paper

### Summary

Physical model tests of floater with full-depth mooring system present obstacles because no tank is sufficiently large to perform model testing in reasonable scale. This paper presents numerical simulation on design method of equivalent truncated mooring systems for model testing of offshore platforms in wave basin. Based on static and dynamic equivalent, two approaches are used to design the truncated mooring systems, respectively. Considering a semi-submersible platform with full-depth and corresponding two equivalent truncated mooring systems, the floater responses and mooring line tensions are compared. The feasibility of model test with equivalent truncated mooring systems is discussed.

*Key words:* truncated; mooring system; equivalent; model testing

### 1. Introduction

Nowadays, the gas and oil industry is concentrating their efforts in developing fields in deeper waters, cumulatively. Within reasonable model scale, physical model testing of floater with full-depth mooring system present obstacles because no tank is sufficiently large to perform model testing of floating platform with complete mooring system in 1500-3000m water depths. The mooring system need to be truncated.

An available method, hybrid approach including combination of model test with truncated set-up and numerical simulation is proposed to deal with the obstacles above [1]. Experimental results from passive truncated mooring system are used for numerical reconstruction and verification in the numerical calculation software. Then the dynamic characteristics of full-depth mooring system could be obtained through the numerical extrapolation [2].

Equivalent design of truncated mooring system is the key aspect for model testing technique. Considering the similarity of static characteristics, several computer codes have been developed. MOOROPT-TRUNC [3] is a special version of MOOROPT combined with MIMOSA and the nonlinear optimization program NLPQL to design truncated mooring and riser system. Zhang et al. [4], Su et al. [5], Udoh [6] developed equivalent truncated mooring

system design codes using various kinds of approaches to calculate the statics of mooring system and employing different optimization algorithms, respectively.

However, the differences of dynamic characteristics between truncated and full-depth mooring system are reflected in the contribution of mooring-induced damping which has huge influence on floater motion responses. The dynamics of truncated mooring lines have been studied by Chen et al. [7]. Su et al. [8] studied the mooring-induced damping based on model tests and numerical simulations.

Thus, both the static and damping characteristics should be considered when the equivalent truncated mooring system is designed. Based on this, an innovative approach has been developed by the author of this paper [9, 10]. Furthermore, the dynamic effect of this innovative equivalent mooring system should be studied.

The objectives for this paper are shown as follows: (1) Analyze the floater motion response and mooring line tension of the platform with different mooring systems; (2) Present the dynamic differences between full-depth and equivalent truncated mooring systems; (3) Discuss the feasibility to perform model testing with the equivalent truncated mooring system.

In this paper, two approaches are used to design the equivalent truncated mooring system. Based on only the static characteristics of mooring system, the Statics Equivalent Truncated Mooring System (SETMS) is designed by the classic method [3]. Considering both the static and damping characteristics of mooring system, an innovative approach [10] is applied to design the Statics and Damping Equivalent Truncated Mooring System (SDETMS). Then, the global responses of a semi-submersible platform with full-depth and corresponding two equivalent truncated mooring systems are compared.

## 2. Equivalent truncated mooring system design

### 2.1 Statics of mooring system

The piecewise extrapolating method is employed to solve the static problem of single mooring line [11]. The top chain AB, the middle wire BC, and the bottom chain OC are divided into  $n_1$ ,  $n_2$ , and  $n_3$  elements, respectively, as shown in Figure 1.

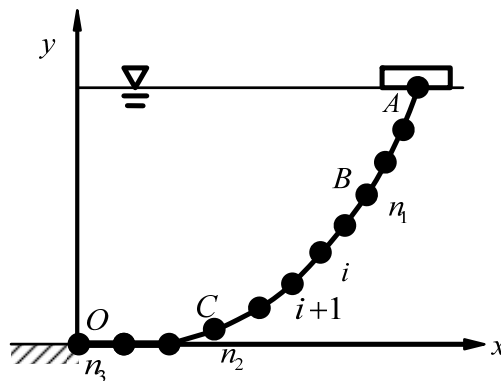


Fig. 1 Elements of mooring line

In order to improve the computational efficiency, golden section search method is adopted in this paper to find out the top angle [9]. It can achieve optimal results by shortening the optimization interval. During each step, the length of new interval is 0.618 times of the former. Thus, this approach has high convergence rate and accuracy.

## 2.2 Mooring-induced damping

Huse and Matsumoto [12, 13] and Huse [14] have studied mooring-induced damping by means of the dissipated energy model.

The dissipated energy  $E$  during one Low Frequency (LF) oscillation of period  $\tau$  is related to the linear coefficient  $B$  by the formula

$$E = \int_0^{\tau} B \left( \frac{dX}{dt} \right)^2 dt \quad (1)$$

where  $X$  refers to the LF component of the surge motions.

Consequently, provided the energy dissipated by the mooring line during one LF surge oscillation can be calculated, the linear damping coefficient can be obtained by

$$B = \frac{E\tau}{2\pi^2 X_0^2} \quad (2)$$

where  $X_0$  is the amplitude of the surge harmonic oscillation.

In this paper, the quasi-static method [10] is employed to calculate the mooring-induced damping.

Consider a discretization of the period  $\tau$  with a time step  $\Delta t = \tau / 2N$ . A total of  $N + 1$  catenary line profiles are computed; the first and the last, respectively, for the near and far positions as shown in Figure 2.

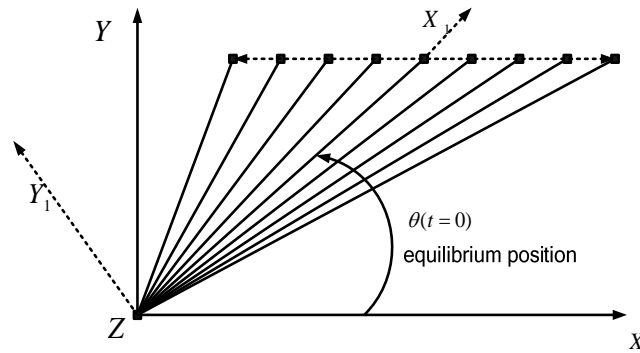


**Fig. 2** Top view of the mooring line positions during one surge oscillation

At each time step, the profile of mooring line could be computed. Consequently, the position of each mooring line element could be considered as a displacement function of time. Then, the velocity and acceleration function can be obtained. Using the Morison Equation, the drag force of each mooring line element can be calculated. Finally, the dissipated energy  $E$ , and the damping can be obtained.

## 2.3 Optimized design criteria

In order to reduce the uncertainties from equivalent truncated to full-depth system, the same motion responses of the floater as would result from the full-depth mooring should be obtained. The equivalent truncated mooring system should preferably have a similarity to the physical properties of the full-depth system. In practice, the design of equivalent truncated mooring system need follow the criteria as below: (1) Model the correct total, horizontal restoring force characteristic. (2) Model representative single line tension characteristics. (3)

Model the correct quasi-static coupling between vessel responses. (4) Model a representative level of mooring system damping.

The classic SETMS can only satisfy criteria (1), (2) and (3). However, all the four criteria can be satisfied by the innovative model SDETMS.

### 2.4 Case study

Based on the full-depth mooring system used for a semi-submersible platform of 1500m water depth in the South China Sea, the SETMS and the SDETMS are designed, respectively.

The layout of mooring lines is shown as Figure 3. Each mooring line has three components: top chain, steel wire and bottom chain.

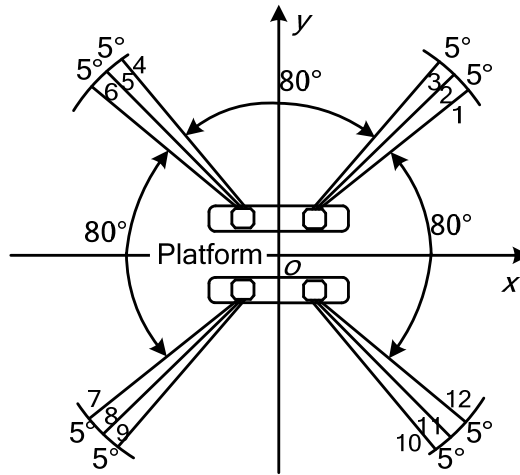


**Fig. 3** Layout of the mooring lines

The Deep Ocean Engineering Laboratory with maximum 10m working water-depth will be established in Dalian University of Technology (DUT). Considering that the reasonable model scale is 1:70, two equivalent truncated mooring systems will be designed for 700m water depth.

The parameters of full-depth mooring line are shown in Table 1. The pretension of each mooring line is 1600 kN.

**Table 1** Parameters of catenary full-depth mooring line

	Diameter (m)	Length (m)	Net Submerged Weight (Nm-1)	Axial Stiffness (MN)
Top Chain	0.084	300	1352.4	620.34
Steel Wire	0.0953	2000	378.8	784.64
Bottom Chain	0.084	1500	1352.4	620.34

During the optimization, the diameter  $D$ , the net submerged weight  $P$ , the length  $L$ , and the axial stiffness  $EA$  of middle wire are considered as variables. In this study, truncation factor ratio is defined as truncated water-depth divides full water-depth.

Considering the optimized design criteria shown above in this paper, based on the similarity of the total horizontal and vertical restoring force, the representative tension of No.5 mooring line and the total mooring-induced damping of mooring system, the weighting

objective functions for designing SETMS and SDETMS are gained, respectively, as shown in Equations 3-4.

$$F_{opt} = w_x \sqrt{\frac{1}{N} \sum_{i=1}^N \left( \frac{Fx_{t,i} - Fx_{f,i}}{Fx_{f,i}} \right)^2} + w_z \sqrt{\frac{1}{N} \sum_{i=1}^N \left( \frac{Fz_{t,i} - Fz_{f,i}}{Fz_{f,i}} \right)^2} + w_T \sqrt{\frac{1}{N} \sum_{i=1}^N \left( \frac{T_{t,i} - T_{f,i}}{T_{f,i}} \right)^2} \quad (3)$$

$$F_{opt} = w_x \sqrt{\frac{1}{N} \sum_{i=1}^N \left( \frac{Fx_{t,i} - Fx_{f,i}}{Fx_{f,i}} \right)^2} + w_z \sqrt{\frac{1}{N} \sum_{i=1}^N \left( \frac{Fz_{t,i} - Fz_{f,i}}{Fz_{f,i}} \right)^2} + w_T \sqrt{\frac{1}{N} \sum_{i=1}^N \left( \frac{T_{t,i} - T_{f,i}}{T_{f,i}} \right)^2} + w_c \sqrt{\frac{1}{K} \sum_{j=1}^K \left( \frac{C_{t,i} - C_{f,i}}{C_{f,i}} \right)^2} \quad (4)$$

where,  $i$  is the step of horizontal offset, and the distance of each step is constant;  $j$  is the frequency of floater harmonic oscillation;  $N$  is the total number of the offset steps,  $K$  is the total number of the frequencies;  $Fx_{t,i}$ ,  $Fx_{f,i}$  are respectively the horizontal restoring force of truncated and full-depth mooring system at position  $i$ ;  $Fz_{t,i}$ ,  $Fz_{f,i}$  are respectively the vertical restoring force of truncated and full-depth mooring system at position  $i$ ;  $T_{t,i}$ ,  $T_{f,i}$  are respectively the top tension of truncated and full-depth mooring line at position  $i$ ;  $C_{t,i}$ ,  $C_{f,i}$  are respectively mooring-induced damping coefficient of truncated and full-depth mooring system at frequency  $j$ ;  $w_x$ ,  $w_z$ ,  $w_T$ ,  $w_c$  are respectively the weighting value of the horizontal restoring force, the vertical restoring force, the representative tension and the mooring-induced damping.

In this paper, after trying and comparing, the weighting values for designing the SETMS are set as 0.4, 0.3, and 0.3, respectively. In addition, the weighting values used to design the SDETMS are set as 0.4, 0.2, 0.2 and 0.2, respectively. During calculation of the mooring-induced damping for optimization, the typical LF periods of surge harmonic oscillation are considered as 30s, 60s, 90s, 120s, 200s, and 300s.

As a result, the final design parameters of the SETMS and the SDETMS are shown in Tables 2-3. The statics and damping characteristics of the SETMS, the SDETMS and the full-depth mooring system are shown in Figures 4-7.

The static characteristics of these three mooring systems fit well. The damping characteristics of full-depth mooring system and SDETMS fit well. However, the damping level of SETMS are relatively smaller.

**Table 2** Parameters of the SETMS

Designation	Diameter (m)	Length (m)	Net Submerged Weight (Nm-1)	Axial Stiffness (MN)
Top Chain	0.084	140	1352.4	620.34
Steel Wire	0.0953	979.35	1519.38	137.20
Bottom Chain	0.084	700	1352.4	620.34

**Table 3** Parameters of the SDETMS

Designation	Diameter (m)	Length (m)	Net Submerged Weight (Nm-1)	Axial Stiffness (MN)
Top Chain	0.084	140	1352.4	620.34
Steel Wire	0.40	816.34	1547.44	1705.23
Bottom Chain	0.084	700	1352.4	620.34

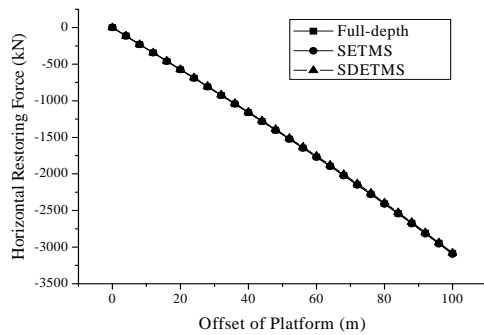


**Fig. 4** The horizontal restoring force of mooring systems

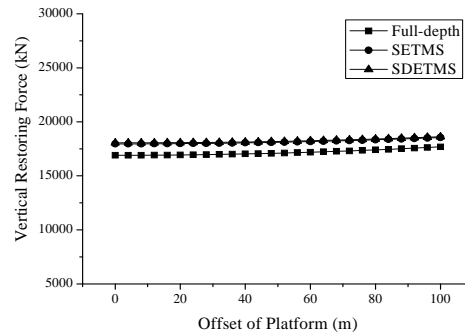


**Fig. 5** The vertical restoring force of mooring systems

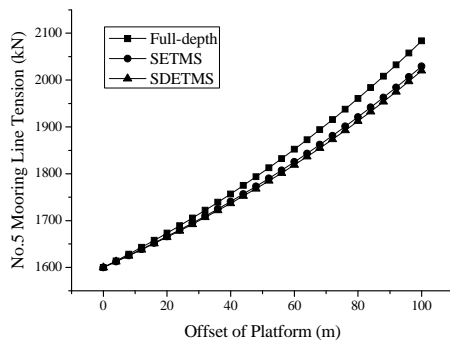


**Fig. 6** The tension of No.5 catenary mooring line

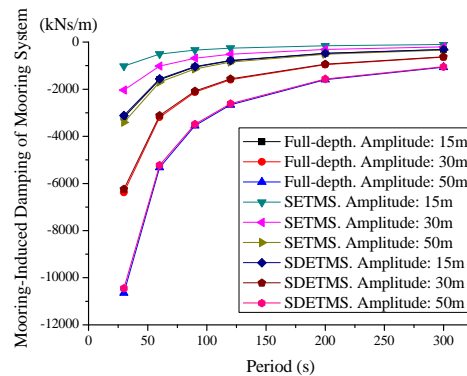


**Fig. 7** The level of mooring-induced damping at different amplitude

### 3. Numerical simulation

To compute the coupled motions, the Cummins's method [15] is applied in this paper. The wave forces on floater are calculated by the boundary element method based on diffraction theory using the commercial program AQWA [16]. The platform structure is treated as a rigid body.

### 3.1 Wave forces

During numerical simulation, the transient wave forces acting on platform in irregular waves are approximately given as [15]:

$$F_i(t) = F_i^{(1)}(t) + F_i^{(2)}(t) \quad (i = 1, 2, \dots, 6) \quad (5)$$

where  $F_i^{(1)}(t)$  and  $F_i^{(2)}(t)$  are the first and second order wave force, respectively. They are shown as follows:

$$F_i^{(1)}(t) = \int_0^t h_i^1(t-\tau)\eta(\tau)d\tau \quad (i = 1, 2, \dots, 6) \quad (6)$$

$$F_i^{(2)}(t) = \int_0^t \int_0^t h_i^2(t-\tau_1, t-\tau_2)\eta(\tau_1)\eta(\tau_2)d\tau_1d\tau_2 \quad (7)$$

where  $h_i^1(t)$  and  $h_i^2(t)$  are the first and second order impulse response functions in time domain, and  $\eta(t)$  is the sea surface elevation.  $h_i^1(t)$  and  $h_i^2(t)$  are given as:

$$h_i^1(t) = \text{Re} \left\{ \frac{1}{\pi} \int_0^\infty H_i^{(1)}(\omega) e^{i\omega t} d\omega \right\} \quad (8)$$

$$h_i^2(t_1, t_2) = \text{Re} \left\{ \frac{1}{2\pi^2} \int_0^\infty \int_0^\infty H_i^{(2)}(\omega_1, \omega_2) e^{i(\omega_1 t_1 + \omega_2 t_2)} d\omega_1 d\omega_2 \right\} \quad (9)$$

where  $H_i^1(\omega)$  and  $H_i^2(\omega_1, \omega_2)$  are the first and second square order transfer functions for wave force in the frequency domain [17].

### 3.2 Governing equation of mooring line

The mooring line is generally presumed to be a completely flexible component during the motion response analysis. The governing equation is proposed by Berteaux [18].

$$m \frac{\partial \vec{V}}{\partial t} = \vec{F}_{Dn} + \vec{F}_{Dt} + \vec{F}_{In} + \vec{F}_{It} + \frac{\partial \vec{T}}{\partial s} + \vec{G} \quad (10)$$

$$\vec{F}_{Dn} = \frac{1}{2} \rho_w C_{Dn} D \left| \Delta \vec{V}_n \right| \Delta \vec{V}_n \quad (11)$$

$$\vec{F}_{Dt} = \frac{1}{2} \rho_w C_{Dt} \pi D \Delta \vec{V}_t \left| \Delta \vec{V}_t \right| \quad (12)$$

$$\vec{F}_{In} = \frac{1}{4} \rho_w \pi D^2 C_{mn} \left( \frac{\partial \vec{U}_n}{\partial t} - \frac{\partial \vec{V}_n}{\partial t} \right) \quad (13)$$

$$\vec{F}_{It} = \frac{1}{4} \rho_w \pi D^2 C_{mt} \left( \frac{\partial \vec{U}_t}{\partial t} - \frac{\partial \vec{V}_t}{\partial t} \right) \quad (14)$$

where  $m$  is the mass of mooring line (per unit length),  $\vec{V}$  is the velocity vector of the mooring line,  $\vec{F}_{Dn}$  is the mooring line normal drag forces (per unit length),  $\vec{F}_{Dt}$  is the mooring line tangential drag forces (per unit length),  $\vec{F}_{In}$  is the mooring line normal inertia forces (per unit length),  $\vec{F}_{It}$  is the mooring line tangential inertia forces (per unit length).  $\frac{\partial \vec{T}}{\partial s'}$  is the partial derivative of mooring line tension  $\vec{T}$  per arc length of extended mooring line  $s'$ , and describes the tension change of a mooring line elementary length  $ds'$ .  $\vec{G}$  is the net weight of mooring line,  $\rho_w$  is the fluid density,  $C_{Dn}$  is the normal drag coefficient,  $D$  is the wire diameter,  $\Delta \vec{V}_n$  is the relative normal velocity of the fluid,  $C_{Dt}$  is the tangential drag coefficient,  $\Delta \vec{V}_t$  is the relative tangential velocity of the fluid,  $C_{mn}$  is the normal added mass coefficient,  $\vec{U}_n$  is the normal velocity vector of fluid at the mooring line direction,  $\vec{V}_n$  is the normal velocity vector of the mooring line,  $C_{mt}$  is the tangential added mass coefficient,  $\vec{U}_t$  is the tangential velocity vector of fluid at the mooring line direction,  $\vec{V}_t$  is the tangential velocity vector of the mooring line.

### 3.3 Coupled analysis of semi-submersible platform and mooring lines

The equation of motion  $\xi(t)$  for the coupled system in time domain is given as follows:

$$(M_{kj} + m_{kj})\ddot{\xi}_j(t) + \int_{-\infty}^t \dot{\xi}_j(\tau)K_{kj}(t-\tau)d\tau + B_{kj}\dot{\xi}_j(t) + C_{kj}\xi_j(t) = F_j(t) + G_j(t) \quad (j=1,2,\dots,6) \quad (15)$$

where  $M_{kj}$  is the mass matrices of the floater,  $C_{kj}$  the hydrostatic restoring stiffness,  $B_{kj}$  is the viscous damping of the system,  $G_j(t)$  is the mooring force,  $F_j(t)$  is the external forces which contain wind loads and wave forces,  $m_{kj}$  and  $K_{kj}(t)$  respectively are the added mass and the retardation function in the time domain.

With the help of convolution integral method [19],  $m_{kj}$  and  $K_{kj}(t)$  can be computer from the added mass  $a_{kj}$  and wave damping  $b_{kj}$  in frequency domain. Assuming the floater motion is related to simple harmonic motion and compared with the motion equation of the floater in frequency domain, any motion of the floater can be described by Equation 15 [20].  $m_{kj}$  and  $K_{kj}(t)$  are given as:

$$m_{kj} = a_{kj}(\infty) \quad (16)$$

$$K_{kj}(t) = \frac{2}{\pi} \int_0^{\infty} b_{kj}(\omega) \cos(\omega t) d\omega \quad (17)$$

Equation 15 can be described as follows:



$$\begin{aligned} \ddot{\xi}_j(t) = & (M_{kj} + m_{kj})^{-1} [F_j(t) + G_j(t) - \\ & \int_{-\infty}^t \dot{\xi}_j(\tau) K_{kj}(t - \tau) d\tau - B_{kj} \dot{\xi}_j(t) - C_{kj} \xi_j(t)] \end{aligned} \quad (18)$$

Equation 18 can be solved by Runge-Kutta method, and the numerical integration could be carried out with the trapezoid rule. The displacement and velocity of the floater at the time step  $t + \Delta t$  are written as:

$$\xi(t + \Delta t) = \xi(t) + \Delta t \dot{\xi}(t) + \Delta t (M_1 + M_2 + M_3) / 6 \quad (19)$$

$$\dot{\xi}(t + \Delta t) = \dot{\xi}(t) + (M_1 + 2M_2 + 2M_3 + M_4) / 6 \quad (20)$$

where  $\Delta t$  is taken as the time step, and

$$M_1 = \Delta t F[t, \xi(t), \dot{\xi}(t)],$$

$$M_2 = \Delta t F[t + \frac{\Delta t}{2}, \xi(t) + \frac{\Delta t \dot{\xi}(t)}{2}, \dot{\xi}(t) + \frac{M_1}{2}],$$

$$M_3 = \Delta t F[t + \frac{\Delta t}{2}, \xi(t) + \frac{\Delta t \dot{\xi}(t)}{2} + \frac{\Delta t M_1}{2}, \dot{\xi}(t) + \frac{M_2}{2}],$$

$$M_4 = \Delta t F[t + \frac{\Delta t}{2}, \xi(t) + \Delta t \dot{\xi}(t) + \frac{\Delta t M_2}{2}, \dot{\xi}(t) + M_3]$$

The function  $F[\Delta t, \xi, \dot{\xi}]$  can be solved using the displacement  $\xi(t)$  and velocity  $\dot{\xi}(t)$  of the floater at the time  $t$ , and the displacement  $\xi(t + \Delta t)$  and velocity  $\dot{\xi}(t + \Delta t)$  of the floater at the time step  $t + \Delta t$  can be computed by using Equations 19-20. The process will be repeated until the calculation is completed.

#### 4. Results and discussion

In this paper, a semi-submersible platform with full-depth mooring system, SETMS and SDETMS is simulated, respectively. The structure of this semi-submersible platform model is mainly composed of two pontoons, four columns, a deck and a derrick. The main parameters of the platform structure are listed in Table 4. The full-depth mooring system, the SETMS and the SDETMS used in the simulation are described and designed in Section 2. The coupled analysis model of platform and mooring lines is shown in Figure 8. The environmental condition in this study is the 100-year return period in the South China Sea, as shown in Table 5. JONSWAP wave spectrum is used during the numerical simulation.

**Table 4** Parameters of the platform structure

Parameters	Value
Deck (m)	$74.42 \times 74.42 \times 8.60$
Column (m)	$17.385 \times 17.385 \times 21.46$
Pontoon (m)	$114.07 \times 20.12 \times 8.54$
Tonnage (kg)	48206800
Centre of gravity from water surface (m)	5.8
Diameter of brace (m)	1.8

**Table 5** Wave parameters

Parameters	Significant wave height (m)	Peak period (s)	Gamma
Value	13.3	15.5	2.4

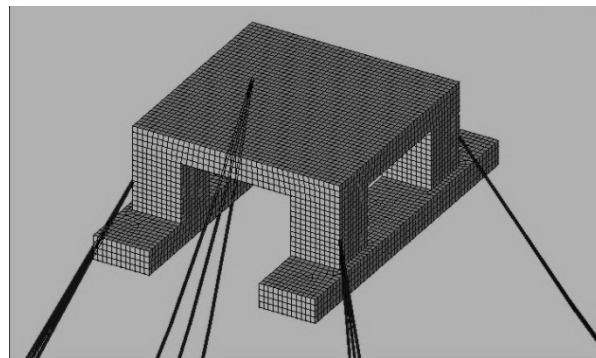


**Fig. 8** The coupled analysis model of platform and mooring lines

Based on the description above, floater responses and mooring line tensions are analyzed. The results are shown as follows.

#### 4.1 Floater motion responses

The floater motion responses are calculated in duration of 3 hours with the incident wave direction as 0 degree. Employing free decay analysis, the natural frequencies of heave and pitch for the moored platform are evaluated as 0.31 rad/s and 0.088 rad/s, respectively. The floater motion (surge, heave and pitch) statistics are described in Tables 6-8. The LF range is 0-0.2 rad/s, and the wave frequency (WF) range is 0.2-1.0 rad/s. The spectra of the whole time series have been calculated with Welch's method <sup>[21]</sup> by use of Fast Fourier Transform (FFT). The representative time series and their spectra are shown in Figures 9-14.

**Table 6** Statistics of surge

Surge (m)	Full-depth	SETMS	SDETMS	
Total	average	48.69	48.61	49.07
	max	74.25	76.98	74.92
	min	-3.93	-3.92	-3.96
	standard deviation	10.43	11.30	10.49
LF	average	48.69	48.60	49.07
	max	72.51	75.08	73.12
	min	-5.89	-5.84	-5.87
	standard deviation	10.23	11.11	10.29
WF	average	0.00	0.00	0.00
	max	7.33	7.34	7.33
	min	-7.81	-7.79	-7.83
	standard deviation	1.99	1.99	1.99

**Table 7** Statistics of heave

Heave (m)	Full-depth	SETMS	SDETMS	
Total	average	4.40	4.32	4.32
	max	9.08	9.22	8.95
	min	-0.36	-0.70	-0.38
	standard deviation	1.55	1.68	1.49
LF	average	4.40	4.32	4.32
	max	4.49	4.41	4.44
	min	4.32	4.24	4.21
	standard deviation	0.00	0.00	0.00
WF	average	0.00	0.00	0.00
	max	4.60	4.81	4.47
	min	-4.77	-5.01	-4.70
	standard deviation	1.55	1.68	1.49

**Table 8** Statistics of pitch

Pitch (degree)	Full-depth	SETMS	SDETMS	
Total	average	2.05	2.10	2.14
	max	10.07	12.93	10.26
	min	-5.20	-7.28	-5.09
	standard deviation	2.19	2.63	2.09
LF	average	2.05	2.10	2.14
	max	7.03	8.74	7.02
	min	-3.43	-3.83	-3.44
	standard deviation	1.42	2.03	1.28
WF	average	0.00	0.00	0.00
	max	5.99	5.92	5.92
	min	-6.05	-5.98	-6.01
	standard deviation	1.67	1.67	1.66

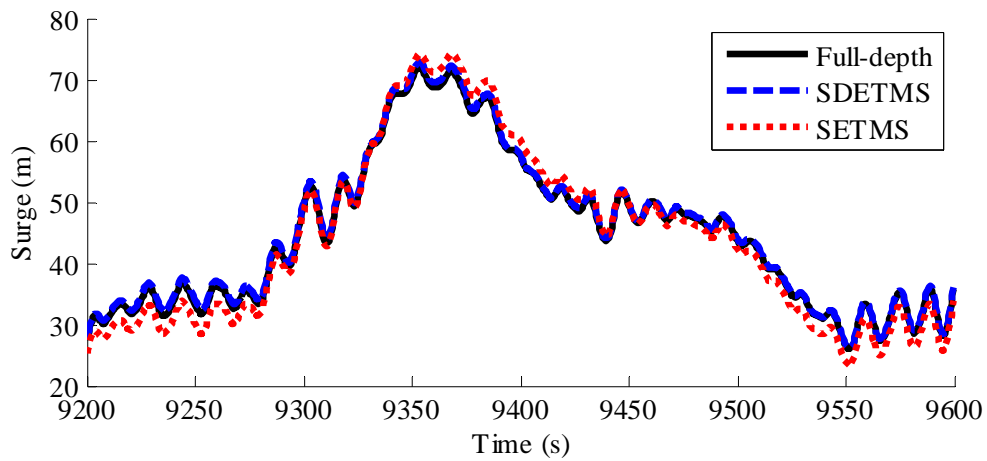


Fig. 9 Representative time series of the surge motion

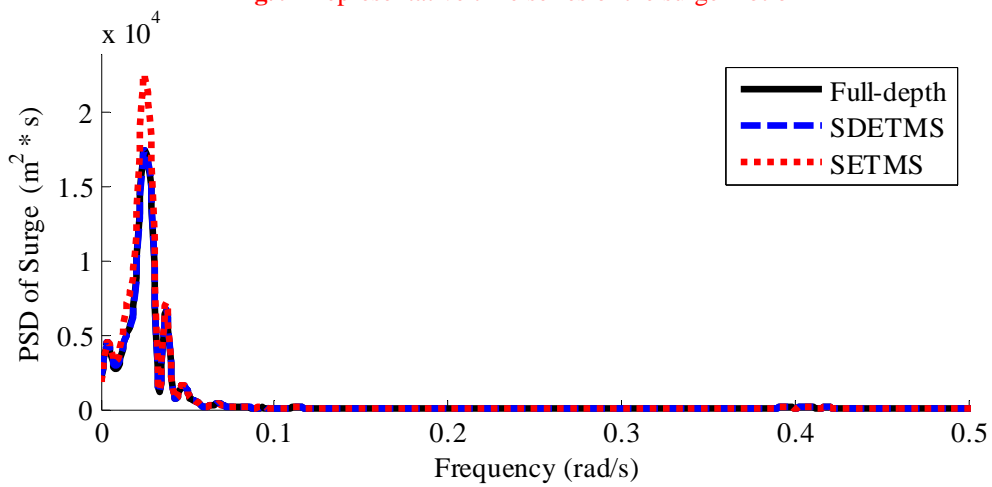


Fig. 10 Spectra of the surge motion

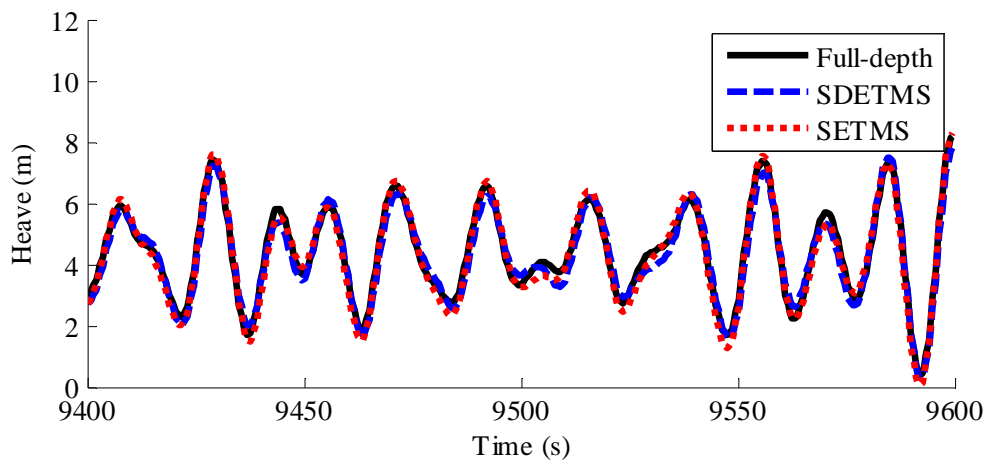


Fig. 11 Representative time series of the heave motion

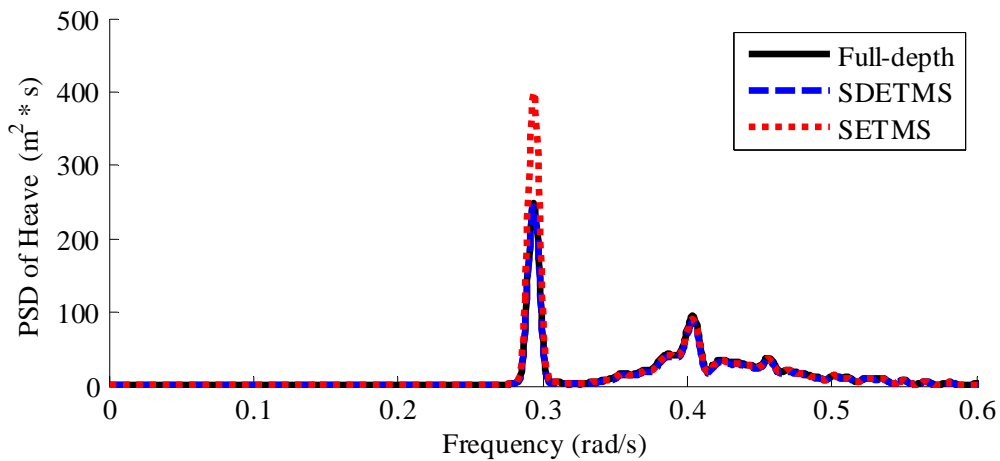


Fig. 12 Spectra of the heave motion

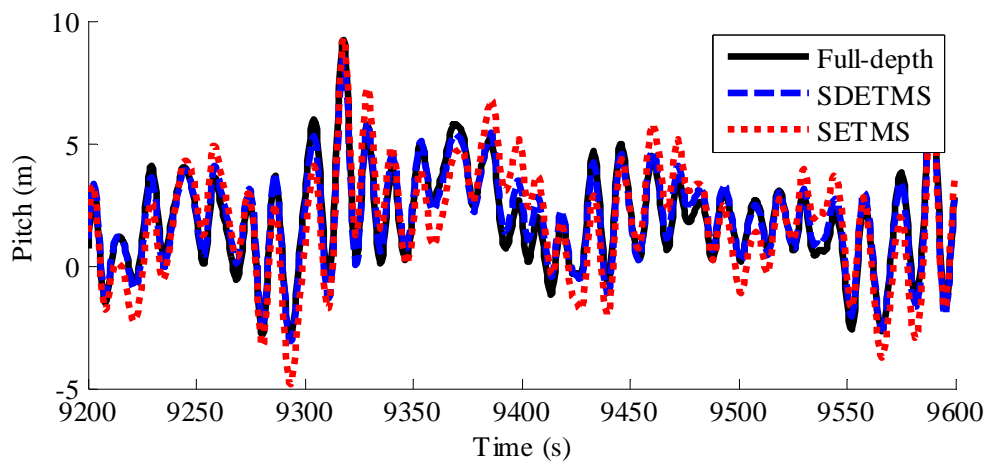


Fig. 13 Representative time series of the pitch motion

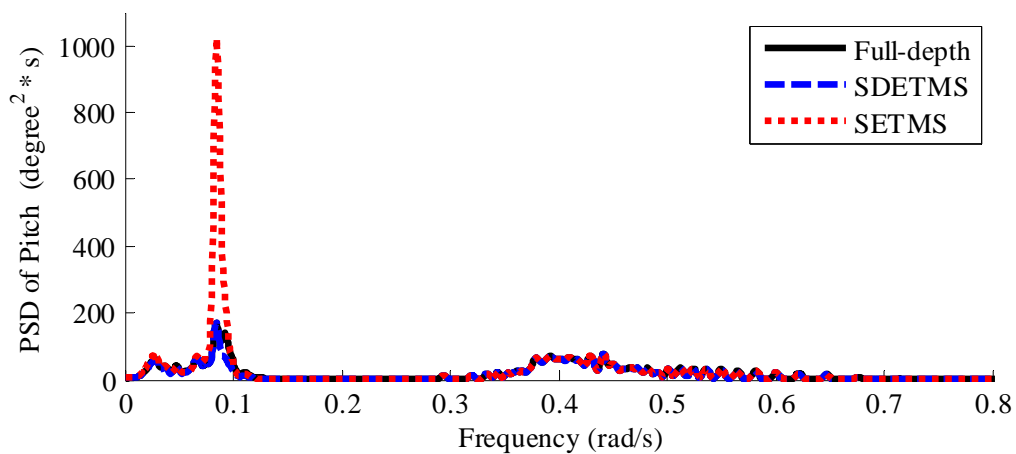


Fig. 14 Spectra of the pitch motion

In this paper, in order to describe easily and clearly, we assume that the floater with the full-depth mooring system, the SETMS and the SDETMS could be expressed as FF, FS and FSD, respectively.

Based on the spectra of surge motion, obviously, the LF motion component is dominant in the surge direction. The dominant frequencies of surge motion are close to the resonance frequencies. Because of the similar damping level of full-depth mooring system and SDETMS, the LF motions of FF and FSD fit well. However, the LF motion of FS is relatively

larger. On the other hand, the WF components of the surge motions of FF, FS and FSD fit well with each other. Based on the statistics of surge motion, for the total and LF motion, the averages of FF, FS and FSD are close, however, the max values, the amplitudes and the standard deviation of FS are larger than those of FF and FSD. For the WF motion component, the statistics of FF, FS and FSD are close.

Based on the spectra of heave motion, obviously, the WF motion component is dominant in the heave direction. The peak frequency of heave motion is at the resonance frequency. Because of the similar damping level of full-depth mooring system and SDETMS, at the peak frequency, the motions of FF and FSD fit well. However, the peak frequency motion of FS is much larger. On the other hand, the LF components of the heave motions of FF, FS and FSD fit well with each other.

Based on the spectra of pitch motion, obviously, the LF motion component is dominant in the pitch direction. The dominant frequencies of pitch motion are close to the resonance frequencies. Because of the similar damping level of full-depth mooring system and SDETMS, the LF motions of FF and FSD fit well. However, the LF motion of FS is relatively larger. On the other hand, the WF components of the surge motions of FF, FS and FSD fit well with each other. Based on the statistics of pitch motion, for the total and LF motion, the max values, the amplitudes and the standard deviation of FS are relatively larger than those of FF and FSD. For the WF motion component, the statistics of FF, FS and FSD are close.

Obviously, in all the directions, the motions of FF and FSD could fit well with each other. On the other hand, the motions of FS are relatively larger, especially at the dominant frequencies near the resonance frequencies.

#### 4.2 Mooring line tension

The mooring line tensions are analyzed in duration of 3 hours with the incident wave direction as 0 degree. The statistics of the representative No.5 mooring line tension are described in Table 9. The LF range is 0-0.2 rad/s, and the wave frequency (WF) range is 0.2-1.0 rad/s. The spectra of the whole time series have been calculated with Welch's method by use of FFT. The representative time series and spectra of the No.5 mooring line are shown in Figures 15-16.

**Table 9** Statistics of No.5 mooring line tension

Tension (kN)	Full-depth	SETMS	SDETMS	
Total	average	1784.2	1764.5	1760.5
	max	2141.9	2021.7	2330.5
	min	1421.0	1479.5	1232.1
	standard deviation	87.6	75.2	147.3
LF	average	1784.1	1764.5	1760.4
	max	1934.0	1889.6	1884.6
	min	1573.2	1577.6	1574.9
	standard deviation	50.0	43.8	41.8
WF	average	0.0	0.0	0.0
	max	254.8	222.9	551.8
	min	-274.7	-205.8	-459.6
	standard deviation	72.0	61.1	141.5

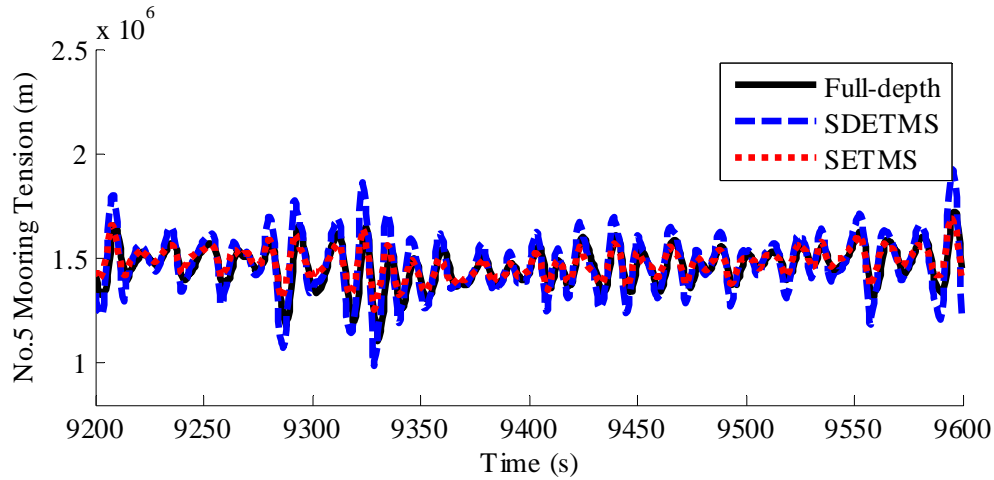


Fig. 15 Representative time series of the No.5 mooring tension

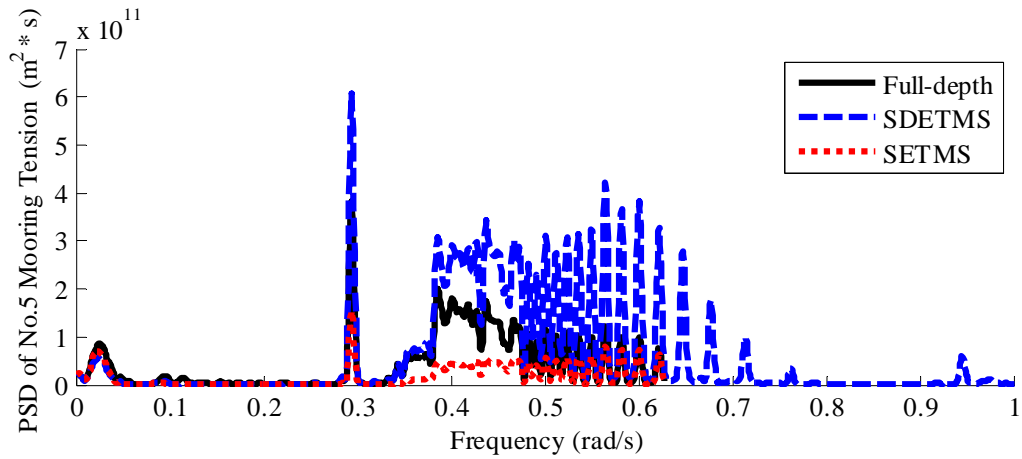


Fig. 16 Spectra of No.5 mooring line tension

In this paper, in order to describe easily and clearly, we assume that mooring line tension of the full-depth mooring system, the SETMS and the SDETMS could be expressed as TF, TS and TSD, respectively.

Based on the spectra of the No.5 mooring line tension, the LF and WF components are both dominant. At LF, the TF, TS and TSD are relatively close. On the other hand, at WF,  $TSD > TF > TS$ . Based on the statistics of the mooring line tension, comparing the total and LF averages of mooring line tension,  $TF > TS > TSD$ . The WF averages of TF, TS and TSD are all zeros. Comparing the LF standard deviation,  $TF > TS > TSD$ . However, comparing the total and WF standard deviation,  $TSD > TF > TS$ . After the damping compensation, the SDETMS is more sensitive to velocity. The floater velocity at WF is relatively higher than that at LF, thus, the WF tension amplitude and standard deviation of SDETMS is relatively larger.

## 5. Conclusions

In this study, the classic SETMS and the innovative SDETMS for deepwater model test are designed. Considering a semi-submersible platform with full-depth mooring system, SETMS and SDETMS, the floater responses and mooring line tensions are compared. The innovative SDETMS could be a better replacement to perform physical model tests. Some useful conclusions can be drawn as follows:

1. The innovative SDETMS designed in this paper can have similar static and damping characteristics with the full-depth mooring system.
2. The mooring-induced damping is important for the floater motion responses at dominant frequencies near the resonance frequency.
3. The motion responses of floater with full-depth mooring system and SDETMS fit well in all directions, at all frequencies even included dominant frequencies near the resonance frequency.
4. Because of the smaller damping level of SETMS, the motion responses of floater with SETMS are relatively larger, especially at dominant frequencies near the resonance frequency.
5. Though the single mooring line tension averages are close, the amplitudes and standard deviations of the three mooring systems can not fit well with each other.

If the objectives of model testing focus on the floater motion responses, the SDETMS could be a good replacement for the full-depth mooring system, so that wave tanks may be sufficiently large to conduct physical model test in reasonable scale.

## ACKNOWLEDGMENTS

This paper was financially supported in part by National Basic Research Program of China (Grant NO. 2011CB013702; 2011CB013703), National Natural Science Foundation of China (Grant NO. 51209037, 51221961), China Postdoctoral Science Foundation Funded Project (Grant NO. 2013T60287), and Fundamental Research Funds for the Central Universities (Grant NO. DUT14RC(4)30).

## REFERENCE

- [1] Stansberg C T, Ormberg H, Oritsland O (2002) Challenges in deep water experiments: hybrid approach. *J Offshore Mech Arct Eng* 124(2):90-96
- [2] Moxnes S, Larsen K (1998) Ultra small scale model testing of a FPSO ship. In: *Proc 17th Int Conf Offshore Mech Arct Eng*, Jul 5-9, Lisbon, Portugal, OMAE98-0381
- [3] Fylling I J (2005) MOOROPT-Trunc – a program for truncation of mooring lines. Trondheim (Norway): Norwegian Marine Technology Research Institute, MARINTEK
- [4] Zhang H, Sun Z, Yang J, et al (2009) Investigation on optimization design of equivalent water depth truncated mooring system. *Science in China series G-physics mechanics & astronomy*, 52(2):277-292
- [5] Su Y, Yang J, Xiao L, et al (2008) Multi-objective optimization design of truncated mooring system based on equivalent static characteristics (in Chinese). *China Offshore Platform*, 23(1):14-19
- [6] Udoh I E (2008) Development of design tool for statically equivalent deepwater mooring systems [Msc thesis]. Texas, USA: Texas A&M University
- [7] Chen X, Zhang J, Johnson P, et al (2000) Studies on the dynamics of truncated mooring line. In: *Proc 10th Int Offshore and Polar Eng Conf*, May 28-Jun 2, Seattle, USA
- [8] Su Y, Yang J, Xiao L (2009) Research on damping of the deepwater truncated mooring line (in Chinese). *China Offshore Platform*, 24(2):23-28
- [9] Fan T, Qiao D, Ou J (2012) Optimized design of equivalent truncated mooring system based on similarity of static and damping characteristics. In: *Proc 22nd Int Offshore and Polar Eng Conf*, June 17-22, Rhodes, Greece
- [10] Fan T, Qiao D, Ou J (2013) Innovative approach to design truncated mooring system based on static and damping equivalent. *Ships and Offshore Structures*, DOI: 10.1080/17445302.2013.867631
- [11] Hao C, Teng B (2003) Static analysis for a non-uniform flexible mooring cable system (in Chinese). *China Offshore Platform*, 18(4): 18-22
- [12] Huse E, Matsumoto K (1988) Practical estimation of mooring line damping. In: *Proc 20th Offshore Tech Conf*, May 2-5, Houston, USA, OTC5676



- [13] Huse E, Matsumoto K (1989) Mooring line damping due to first- and second-order vessel motion. In: Proc 21st Offshore Tech Conf, May 1-4, Houston, USA, OTC6137
- [14] Huse E (1991) New developments in prediction of mooring system damping. In: Proc 23rd Offshore Tech Conf, May 6-9, Houston, USA, OTC6593
- [15] Cummins W E (1962) The impulse response function and ship motions. Washington, DC: DTMB, Report No. 1661
- [16] AQWA User Manual (2006) AQWA-LINE manual. Horsham: Century Dynamics
- [17] Teng B, Li Y, Dong G (1999) Second-order wave force on bodies in bi-chromatic waves. *Acta Oceanol Sin*, 21(2):115-123
- [18] Berteaux H O (1976) Buoy engineering. New York: Wiley Interscience
- [19] Li B (2011) Investigation on hydrodynamics and motion performance of an innovative deep draft multi-spar platform [PhD thesis]. Harbin Institute of Technology
- [20] Li Y, Teng B (2002) Wave action on maritime structures (in Chinese). 2nd ed. Beijing: Ocean Press
- [21] Welch P D (1967) The use of fast fourier transform for the estimation of power spectra: a method based on time averaging over short, modified periodograms. *IEEE Trans Audio Electroacoustics*, AU-15:70-73.

Submitted: 15.02.2014. Tianhui Fan, Jinping Ou  
State Key Laboratory of Coastal and Offshore Engineering,  
Accepted: 15.09.2014. Dalian University of Technology, Dalian, China  
DongSheng Qiao, qds903@163.com  
Deepwater Engineering Research Center,  
Dalian University of Technology, Dalian, China  
*Address: Faculty of Infrastructure Engineering, Building 4#, Room 306,  
Dalian University of Technology, Linggong Road No.2, Dalian, Liaoning,  
China, 116024*